JOURNAL OF AIRCRAFT
Vol. 38, No. 3, May–June 2001

Periodic Excitation for Jet Vectoring and Enhanced Spreading

LaTunia G. Pack* and Avi Seifert†
NASA Langley Research Center, Hampton, Virginia 23681

The effects of periodic excitation on the evolution of a turbulent jet were studied experimentally. A short, wide-angle diffuser was attached to the jet exit, and excitation was introduced at the junction between the jet exit and the diffuser inlet. The introduction of high-amplitude periodic excitation at the jet exit enhances the mixing and promotes attachment of the jet shear layer to the diffuser wall. Vectoring is achieved by applying the excitation over a fraction of the circumference of the circular jet, enhancing its spreading rate on the excited side and its tendency to reattach to that side. Static-deflection studies demonstrate that the presence of the wide-angle diffuser increases the effectiveness of the added periodic momentum caused by a favorable interaction between the excitation, the jet shear layer, and the diffuser wall. This point was further demonstrated by the evolution of a wave packet that was excited in the jet shear layer. Strong amplification of the wave packet was measured with a diffuser attached to the jet exit. The turbulent jet responds quickly (10–20 ms) to step changes in the level of the excitation input. The response scales with the jet-exit velocity and is independent of the Reynolds number. Jet deflection angles were found to be highly sensitive to the relative direction between the excitation and the jet flow and less sensitive to the excitation frequency. Significant jet deflection angles were obtained for a diffuser length of one-half to two diameters and for diffusers with half-angles greater than 15 deg.

Nomenclature

A_{jet}	=	jet cross-section area, πr^2
A_{slot}	=	active slot area, $\pi h(2r+h)/4$
$\langle c_\mu \rangle$	=	periodic momentum coefficient, $J'/(\rho A_{\text{jet}} U_e^2)$
D	=	jet diameter, 39 mm
F^+	=	reduced frequency, fL/U_e
f	=	excitation frequency, Hz
h	=	slot width or height, 1 mm
J'	=	periodic momentum at slot exit, $\rho_{\text{Aslot}} u'^2_{\text{slot}}$
K	=	1000
L	=	distance from jet exit to diffuser exit, measured along diffuser wall
p	=	pressure
Re_D	=	Reynolds number based on diameter, $U_e D/v$
r	=	jet radius, 19.5 mm
S_{tD}	=	Strouhal number based on jet diameter, fD/U_e
$S_{t\theta}$	=	Strouhal number based on momentum thickness, $f\theta/U_e$
t	=	time
U	=	jet mean velocity
U_c	=	wave packet convection velocity
u'	=	rms of the velocity fluctuations
V	=	y velocity component
v	=	kinematic viscosity
x	=	axial direction, $x = 0$ at jet exit and diffuser inlet
y	=	vertical direction, $y = 0$ at jet centerline
y_c	=	jet center of momentum
z	=	horizontal direction, $z = 0$ at jet centerline
δ	=	jet deflection angle, deg
θ	=	jet two-dimensional shear-layer momentum thickness
ρ	=	density
ϕ	=	diffuser half-angle, deg

Subscripts

d	=	derectified
e	=	conditions at jet exit
i	=	index denoting z location
plane	=	profiles of an entire jet cross section
profile	=	jet-profile at $z/D = 0.0$
slot	=	condition at slot exit
tog	=	actuator toggle time

I. Introduction

TURBULENT jets are of significant engineering relevance for aerospace and mechanical applications (jet engines, combustion chambers, etc.) and to the environment (chimney stacks). As such, they have been extensively investigated over the last few decades. Controlled excitation was initially used in order to clarify the importance of coherent structures on the evolution of transitional and turbulent jets.[1,2] Research efforts were devoted to understanding the importance of coherent structures in noise generation and jet spreading. Controlled, far-field, acoustic excitation was used in most of these studies to generate the jet coherent structures, owing to the strong receptivity of the jet lip. The limitations of acoustic excitation (power requirements, weight, applicability, and efficiency) led researchers to examine other methods for jet flow control. These methods include cross-stream blowing,[3] counterflow,[4–6] "flip-flop" jets,[7] and high-amplitude periodic excitation.[8] Davis[3] introduced cross-stream steady blowing through two circular tubes positioned on each side of the jet exit. It was shown that the radial introduction of steady momentum enhanced mixing for secondary jet momentum coefficients lower than 0.56%. For higher momentum coefficients a mean flow distortion was generated. Vectoring was not seen because both control jets operated simultaneously.

Strykowski and Wilcoxin[4] attached a diffuser, 1.0–2.25 jet diameters long, to a low-speed, circular jet and applied suction around the jet circumference. The application of suction modifies the jet-exit velocity profile and turns it absolutely unstable for suction velocities greater than 31.5% of the jet centerline velocity.[9] Enhanced mixing or vectoring could be achieved depending on the fraction of the jet circumference to which suction was applied. Thrust vectoring was demonstrated at a Mach number of 2.0, using the jet-suction diffuser arrangement when suction was applied over a fraction of the circumference of a circular jet[5] or along one wall of a rectangular jet.[6] Jet deflection angles were determined by flow visualization. Because the diffuser angles were relatively small, a bistable situation was

Presented as Paper 99-0726 at the 37th Aerospace Sciences Meeting, Reno, NV, 11–14 January 1999; received 4 August 1999; revision received 8 February 2000; accepted for publication 8 September 2000.

*Research Engineer, Physics and Control Branch. Member AIAA.
†Currently Senior Lecturer, Department of Fluid Mechanics and Heat Transfer, Faculty of Engineering, Tel-Aviv University, Ramat-Aviv 69978, Israel. Senior Member AIAA.

encountered because the jet had a tendency to naturally reattach to the diffuser walls.

Raman and Cornelius[7] placed two flip-flop jets[10] on opposite sides of a low-speed rectangular jet to generate alternating directed forcing with a 180-deg phase shift between the control jets. This generated a flapping mode that enhanced the mixing of the primary jet flow. Smith and Glezer[8] used a narrow excitation slot positioned close to the exit of a high-aspect-ratio low-speed rectangular primary jet. The interaction between the jet and the high-frequency and high-amplitude excitation vectored the primary jet. It is not known if the primary jet was laminar, transitional, or turbulent. The magnitude of the fluctuating excitation momentum at the slot exit was not specified. It was concluded[8] that the mechanism responsible for the jet deflection was a low-pressure region generated by the excitation between the primary jet and the excitation slot. More recently, Davis and Glezer[11] forced a low-speed circular jet using up to nine actuators situated around the jet circumference. When six of the actuators operated, generating $\langle c_\mu \rangle \cong 25\%$ an approximate deflection angle of 6 deg was achieved. This $\langle c_\mu \rangle$ estimation was performed by the present authors using the data provided in Ref. 11 and in Figs. 5 and 14 in Ref. 12. A recent numerical simulation[13] showed that the presence of a confinement on one side of a jet, when suction is applied at the confined side, causes enhanced production of coherent structures and jet deflection toward the confined side.

The aim of the present investigation is vectoring and enhanced spreading of a circular, turbulent jet. The mechanism used for vectoring the jet is zero-mass-flux periodic excitation. Periodic excitation is used because of its demonstrated ability to effectively control separation on airfoils. Experiments performed on a variety of airfoils, over a large range of Reynolds and Mach numbers,[14–16] indicate that periodic excitation can be used to effectively delay turbulent boundary-layer separation and reattach separated flows. The introduction of periodic excitation slightly upstream of the boundary-layer separation location enhances mixing between the high-momentum fluid away from the surface and the low-momentum fluid near the surface. Periodic excitation is more efficient than steady suction and two orders of magnitude more efficient than steady blowing at controlling separation.[14–16]

The three main advantages of using periodic excitation for jet flow control are 1) the potential weight reduction of a mechanical thrust vectoring system, 2) the ability to change the aerodynamic forces and moments quickly without generating prohibitive inertial loads on the structure, and 3) the demonstrated superior efficiency of the method compared to steady suction or blowing.

The present paper demonstrates the enhanced controllability of a turbulent jet when a short, wide-angle diffuser is attached at the jet exit and periodic excitation is introduced at the juncture between the jet exit and the diffuser inlet. A preliminary parametric study shows how jet deflection angles were affected by the diffuser geometry (i.e., diffuser length and diffuser half-angle) and by variations in the control inputs (such as excitation frequency, its periodic momentum, and the relative orientation of the excitation). The response of the jet to generic control inputs was also investigated. The relationship between the present control strategy and the flow stability was examined in order to understand how the excitation interacts with the jet flow and the diffuser walls.

II. Experiment Setup

A. Jet

The jet facility consists of a dc fan connected to a 76.2-mm-diam settling chamber, leading to a 3.15 : 1 contraction that is followed by a straight aluminum pipe with an inside diameter of 38 mm and an outside diameter of 40 mm. The thickness of the pipe wall, at the jet exit, was machined to bring it gradually to 0.5 mm in order to reduce the gap between the jet flow and the excitation slot. The jet-exit diameter is therefore 39 mm (Figs. 1a and 1b). The jet was surrounded by a segmented slot, 1 mm wide. Each segment of the slot was connected to a cavity allowing independent excitation of every 45 deg of the jet circumference. The excitation was introduced through the slot surrounding the upper 90 deg of the jet circumference (Figs. 1a and 1b). Trip grit (#36) was placed inside the aluminum pipe, 200 mm from the jet exit, to ensure that the flow at the jet exit was turbulent over the velocity range of interest (8–18 m/s).

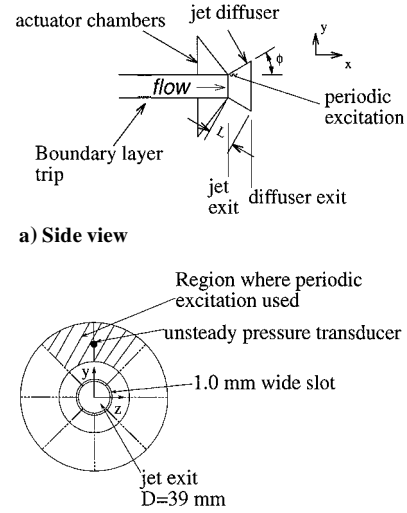

Fig. 1 Schematic description of the jet.

B. Diffusers

A short, wide-angle diffuser could be attached to the exit of the jet. The effect of diffuser length on jet deflection angle was studied by testing diffusers with a half-angle of $\phi = 30$ deg and lengths of $L = 0.58D$, $1.0D$, and $1.85D$. The effect of diffuser half-angles of $\phi = 15$, 22.5, and 30 deg (with a fixed $L = 0.58D$) on jet deflection angle was also examined. The $\phi = 30$ deg, $L = 1.85D$ diffuser was designed such that periodic excitation could be introduced in the streamwise and cross-stream direction.

C. Actuator

A zero-mass-flux piezoelectric actuator, which resonated near 700 Hz, was used to generate the periodic excitation. The velocity fluctuations u' exiting the slot were measured using a hot wire positioned at the slot exit. Because hot wires cannot sense flow direction, the velocities obtained at the slot exit, in the absence of jet flow, had to be derectified using a tested procedure.[16] The maximum u' of the actuator $u'_{\max}$, when operated at 700 Hz using streamwise excitation, is about 18 m/s. The $u'_{\max}$ is about 10% lower when cross-stream excitation is used. When the actuator operated at 350 Hz, using streamwise excitation $u'_{\max}$ was about 9 m/s. The effect of the jet-exit velocity or the presence of a diffuser changes the slot u' by less than 5%. The hot-wire measurements were used to determine the (linear) relationship between the actuator input voltage and the slot velocity fluctuations. This calibration was used to determine u' when the hot wire was removed. In addition, a dynamic pressure transducer was installed in the actuator cavity to monitor its output and provide a phase reference (Fig. 1b).

D. Instrumentation and Data Acquisition

Most of the jet flowfield measurements were acquired using a single hot wire. Hot-wire calibrations were performed at the core of the jet exit, and data repeatability was checked often. The data-acquisition sequence included measuring the jet baseline flow before and after acquiring controlled jet data. A check of the two baseline data sets also served as a check of the hot-wire calibration. In addition, data were acquired using a five-hole probe.[17]

Hot-wire, static, and dynamic pressure data were acquired using a 16-bit A/D converter. The sampling rate of the dynamic data was either 6 or 12 kHz, and the data were low-pass filtered at the sampling rate divided by 2.56. The frequency response of the hot-wire and dynamic pressure transducer was better than 20 kHz. The hot-wire and the five-hole probe were mounted on a three-axis traverse system. All of the experimental instruments were interfaced with a desktop computer.

E. Experimental Uncertainty

The velocities measured with the hot wire are accurate to within 2%. The hot-wire position (x, y, or z) is accurate to within ± 0.04 mm, the Re_D is accurate to within 3%, the $\langle c_\mu \rangle$ is accurate to within 15%, and the jet deflection estimates are accurate to within ± 0.5. deg.

III. Discussion of Results

A. Baseline Jet

1. *Reynolds-Number Effect*

The flow-field of the baseline jet was documented over the widest possible range of Reynolds numbers to verify that the flow was turbulent and to assess the effect of Reynolds number, especially in the near-exit region. Turbulent, Reynolds-number independent flow was desired for this flow control experiment to eliminate transition effects, reducing the number of variables and ensuring that the results would be applicable to higher Reynolds numbers. By tripping the flow five diameters upstream of the jet exit, it was ensured that the effects produced by using periodic excitation were not transition related. The mean and fluctuating velocity profiles close to the jet exit, at $x/D = 0.1$, are presented in Figs. 2a and 2b. The shapes of the mean velocity profiles are identical over the Reynolds-number range tested. The peak turbulence level in the shear layer increases slightly as the Reynolds number decreases (Fig. 2b). The differences in the turbulence levels for the three Reynolds numbers could be caused by a partially developed flow at the lowest Reynolds number. The spectra of the velocity fluctuations measured at $y/r = 0.97$ (Fig. 2c) indicate slight differences in the spectra of the lowest Reynolds number. A line with a slope of $-5/3$ is also shown on Fig. 2c. It helps demonstrate that for the three Reynolds there is a range of frequencies that agree with the Kolmogorov law for the inertial subrange. However the flow at $Re_D = 2.1 \times 10^4$ cannot be considered fully developed turbulent because some differences caused by the Reynolds number can be identified. The two-dimensional momentum thickness of the jet shear layer θ at $x/D = 0.1$ doubles between $U_e = 6$ and 8 m/s, indicating that transition from laminar to turbulent flow occurs. Between 8 and 18 m/s ($Re_D = 2.1 \times 10^4$–4.7×10^4), the θ has a mean value of 1.68 mm $\pm 3.0\%$.

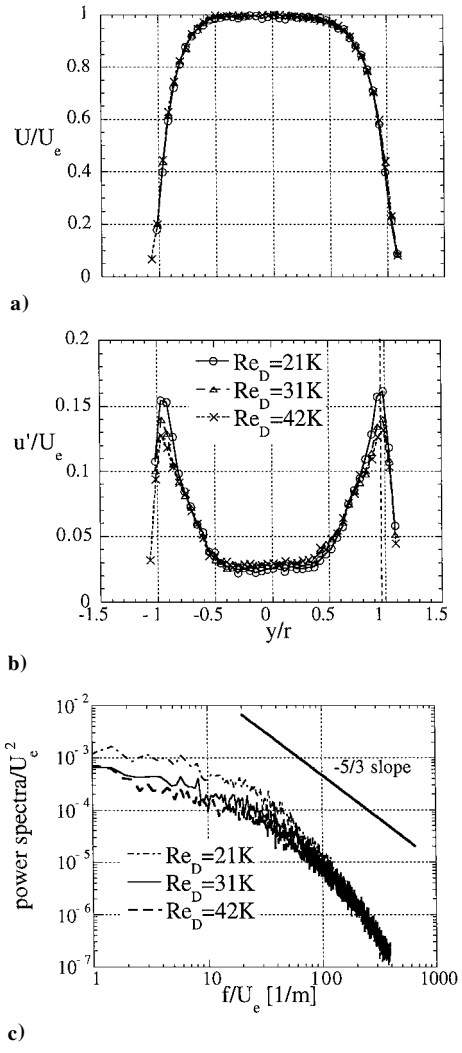

Fig. 2 Baseline a) U and b) u' velocity profiles and spectra at $y/r = 0.97$ (c) at $x/D = 0.1$ and $z/D = 0.0$. - - - -, on b) indicates y location of spectra shown in c).

2. *Effects of the Attached Diffuser*

The flowfield near the exit of the baseline jet, with and without diffusers attached, was carefully examined. It is shown that the presence of the diffuser has very little effect on the shape of the mean velocity profiles (Fig. 3). The initial thickness of the two-dimensional jet shear layer θ is about $D/25$ (Fig. 4). This value is significantly higher than the published values for laminar jet-exit boundary layers[4] ($D/200$) as well as for turbulent boundary layers[18] ($D/160$). However, the elimination of Re_D effects seems more important for the present investigation than allowing a closer similarity to a two-dimensional mixing layer. A significant increase in θ occurs between the jet exit and $x/D = 0.2$, with a diffuser present (Fig. 4). Further downstream, the jet spreads linearly. The spreading rate of the jet shear-layer momentum thickness $d\theta/dx$ increases from 0.03 to 0.031 when a diffuser is placed at the jet exit (Fig. 4). The values of the present $d\theta/dx$ are about 10% lower than those found by others[18] for a jet with turbulent boundary layers at the nozzle. The effect of the increased initial thickness of the jet shear layer is to increase the required input momentum for a required modification (in this case jet deflection angle) based on airfoil separation control experiments. The high initial momentum thickness is also expected to reduce the most amplified frequency, based on linear two-dimensional mixing-layer theory. The velocity profiles in the

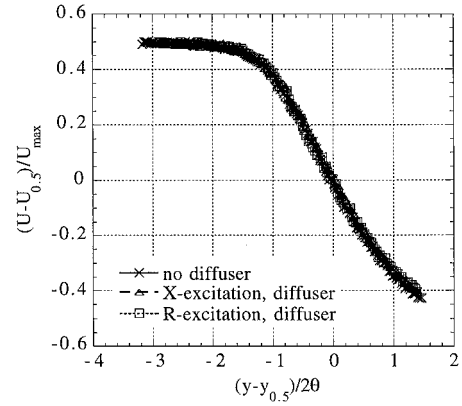

Fig. 3 Diffuser effect on baseline velocity profiles, $x/D = 1.6$, $z/D = 0.0$, $Re_D = 3.1 \times 10^4$, $\phi = 30$ deg, and $L = 1.85D$.

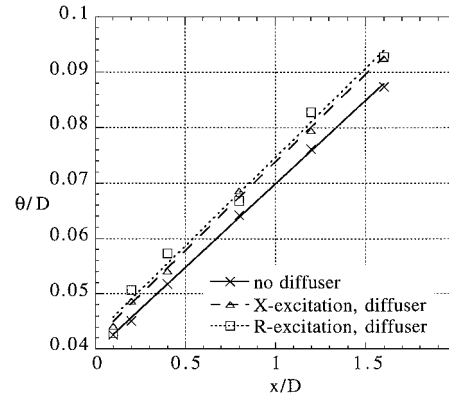

Fig. 4 Diffuser effect on the shear-layer momentum thickness close to the jet exit. $Re_D = 3.1 \times 10^4$, $\phi = 30$ deg, and $L = 1.85D$.

near-exit region of the jet are not self-similar, nor is the flow parallel. This indicates that linear, parallel stability approaches are not applicable to this type of flow. Furthermore, the challenge here is to generate a mean flow modification that is inherently nonlinear and nonaxisymmetric.

B. General Aspects of Periodic Excitation

1. *Baseline and Controlled Cross-Section Planes*

Hot-wire surveys of the jet flowfield were made at a cross-stream plane at $x/D = 2.5$ and $Re_D = 3.1 \times 10^4$. The baseline mean velocity contours are shown in Fig. 5a. The circular shape of the baseline contours indicates that the flow is axisymmetric. The maximum turbulence level of the baseline jet is about 15%, and the u' contours are also axisymmetric (not shown). Controlled mean velocity contours, using streamwise excitation with a diffuser attached, are shown in Fig. 5b. The excitation is introduced through the upper 90 deg of the slot around the jet circumference. The enhanced mixing between the excited jet and the surrounding ambient flow leads to higher flow rates on the upper side of the jet. The increased mixing causes the mean velocity contours to be elongated in the vertical y direction and contracted in the horizontal x direction compared to the baseline. The spanwise contraction indicates that the jet is also vectored as a result of forces exerted by the upper 90 deg of the diffuser wall and not only as a result of enhanced mixing. The center of the jet linear momentum shifts upward, indicating that the jet flow is vectored up by about 6 deg (analysis to follow). The maximum fluctuating velocity of the controlled jet using streamwise excitation and a diffuser (not shown, Ref. 19) is about 0.18–$0.21U_e$ and has a horseshoe-like shape. The data of Fig. 5b were repeated without a diffuser attached at the jet exit (Fig. 5d). A significantly smaller modification of the jet cross section was obtained. A small increase in the jet spreading rate (compared to the baseline) could be observed in the excited shear layer. The jet is deflected only by 2.2 deg. The presence of a diffuser wall at the jet exit significantly enhances the effectiveness of the streamwise excitation. Controlled excitation was also introduced in the cross-stream direction (Fig. 5c). This mode of high-amplitude excitation results in a deflection of the jet away from the excitation slot. The jet cross section is now elongated in the spanwise direction. This type of excitation does not increase the spreading rate nor the turbulence level as much as the streamwise excitation does. Similar excitation modes were identified by Smith and Glezer,[8] as the *push* and *pull* modes. As will further be shown, the presence of a diffuser at the jet exit significantly enhances the effectiveness of the streamwise excitation. The evolution of the cross-stream excited jet without a diffuser attached has not been studied yet.

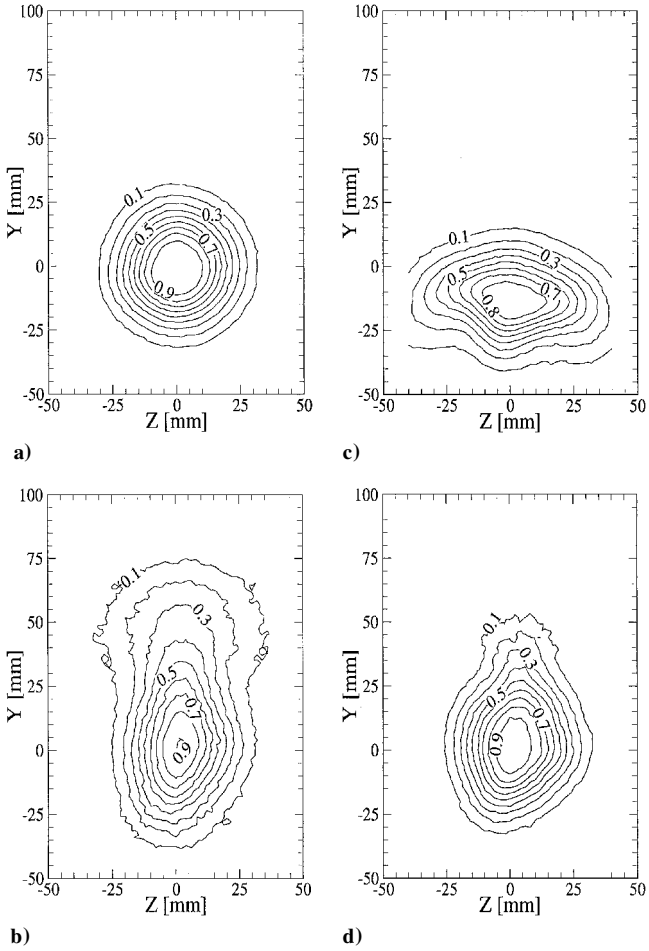

Fig. 5 Mean velocity contours measured at x/D = 2.5 and Re_D = 3.1×10^4 for a) baseline, streamwise excitation, b) $\langle c_\mu \rangle$ = 3.3%, F^+ = 2.3, L = 1.0D diffuser, c) cross-stream excitation $\langle c_\mu \rangle$ = 3.3%, F^+ = 4.2, L = 1.85D diffuser, and d) streamwise excitation, $\langle c_\mu \rangle$ = 3.3%, no diffuser.

2. *Determination of Jet Deflection Angle*

Jet deflection angles could be estimated from the ratio of the y to x total linear momentum at the exit plane of a control volume including the jet, diffuser, and excitation slots. This requires the measurement of at least two velocity components at the control volume exit plane. Although data of complete cross-section planes provide a more comprehensive description of the jet flow, the time required to acquire the data is excessive, and the amount of data is enormous. A parametric study at this pace would have been prohibitive. An examination of the shape of the cross-section planes presented in Figs. 5 indicates that $z = 0$ is a symmetry line. The question we attempt to answer is could data acquired along this line, using a single hot-wire, provide data that are representative of the entire jet cross section. To address this issue, we first acquired several profiles using a five-hole probe.[17] This probe enables the acquisition of three velocity components and provides an independent measure of jet deflection angles. The jet deflection angles from the five-hole probe data were computed using the local flow angle

$$\delta_{5,j} = \tan^{-1}(V_j/U_j) \tag{1a}$$

inserted into the y component of the linear momentum equation applied to a control volume in the form

$$\delta_{5,\text{profile}} = \frac{\sum_j U_j^2 \delta_{5,j}}{\sum_j U_j^2} \tag{1b}$$

where j is an index in the vertical direction y. Data where the local velocity U were greater than $0.125U_e$ were included in the average (filled triangles in Fig. 6).

Deflection angles based on hot-wire data were calculated in the following manner. The total streamwise linear momentum at a given spanwise location z/D was computed using

$$M_i = \int U^2 \, dy \tag{2a}$$

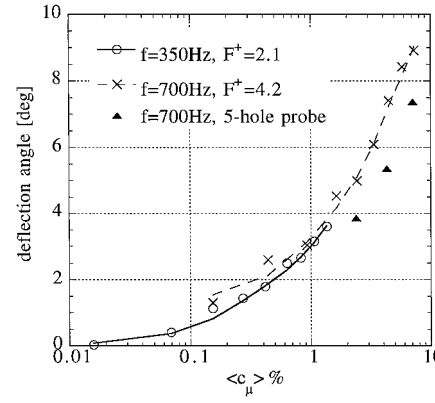

Fig. 6 Effect of the excitation frequency on jet deflection angles. $Re_D = 3.1 \times 10^4$, x/D = 2.5, z/D = 0.0, ϕ = 30 deg, L = 1.85D diffuser.

where U is the jet mean velocity at a given vertical y position in the profile and i is an index denoting the increment in the horizontal z direction. The data were integrated in y over the valid range of the hot-wire calibration velocities. The center of linear momentum of the jet at a given spanwise location z/D was determined by

$$y_{c,i} = \frac{\int U^2 y \, dy}{\int U^2 \, dy} \tag{2b}$$

The deflection angle based on one profile measured at $z/D = 0$ is defined as

$$\delta_{\text{profile}} = \tan^{-1}(y_{c,\text{profile}}/x) \tag{3}$$

where x is the distance from the jet exit to the measuring station. Equation (3) could be considered an approximation of Eq. (1b), where the local deflection angle is equal to the geometric angle. Complete cross-section planes of hot-wire data were also used, in the following manner, to evaluate the jet deflection angle. The center of linear momentum of the jet at a given cross-stream location x/D was determined using

$$y_{c,\text{plane}} = \frac{\sum_i M_i y_{c,i}}{\sum_i M_i} \tag{4}$$

The deflection angle based on a whole cross-section plane was determined by assuming that the jet began deflecting at $x/D = 0.0$ and computing jet deflection angle δ_{plane} using

$$\delta_{\text{plane}} = \tan^{-1}(y_{c,\text{plane}}/x) \tag{5}$$

where x is the distance from the jet exit to the measuring station. A comparison between the deflection angle computed using single hot-wire profiles measured on the jet plane of symmetry δ_{profile} and the deflection angles computed using entire cross-section planes δ_{plane} were made. The deflection angles computed using Eqs. (3) and (5) agree to within ±0.5 deg (Fig. 7, Ref. 19). The deflection angles obtained with the five-hole probe are lower by 0.5 to 1.25 deg than the deflection angles based on single hot-wire profiles (Fig. 6). An observation that the jet deflection angle decreases with x/D (Fig. 7, Ref. 19) implies that the jet actually started to deflect about one-diameter upstream of the jet exit. This explains the higher deflection angles obtained using the hot-wire data (Fig. 6). The close agreement between the three methods in determining the jet deflection angle allows us to use the most efficient method, i.e., single hot-wire profiles measured at $z/D = 0.0$ and $x/D = 2.5$. This location always corresponds to a plane of symmetry of the excited flow. Furthermore, the jet deflection angles to be presented should be used as trends of the effects of the various parameters, whereas absolute angles should preferably be measured with a force balance.

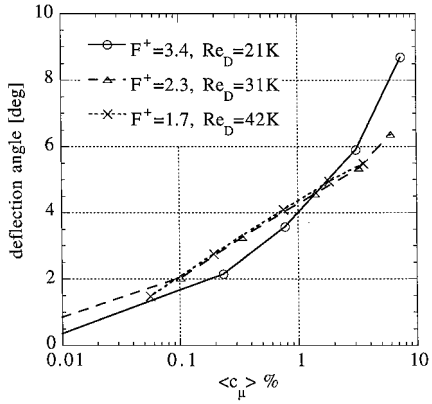

Fig. 7 Effect of Re_D on jet deflection angles measured at $x/D = 2.5$ and $z/D = 0.0$. $\phi = 30$ deg, $L = 1.0D$ diffuser.

C. Parametric Study

1. *Effect of Reynolds Number*

To study the effect of Reynolds number on the evolution of the controlled jet, data were acquired at three jet speeds corresponding to $Re_D = 2.1 \times 10^4$, 3.1×10^4, and 4.2×10^4. Streamwise excitation with a frequency of 700 Hz was used for this study. As will be shown later, the effect of the corresponding change in F^+ with Re_D is small. Figure 7 shows jet deflection angles vs periodic momentum coefficient $\langle c_\mu \rangle$ for the three Reynolds numbers tested. The jet deflection angles for the two higher Reynolds numbers are in excellent agreement, indicating weak Reynolds-number dependence. At $Re_D = 2.1 \times 10^4$ the jet has lower deflection angles for lower $\langle c_\mu \rangle$ and higher deflection angles for $\langle c_\mu \rangle$ above 2%. This could be a result of the developing nature of the turbulent boundary layer upstream of the jet exit as shown for this Re_D in Figs. 2b and 2c.

2. *Effect of the Excitation Frequency*

To study the effects of F^+ without varying Re_D, the actuator was operated at two frequencies, 700 Hz (actuator resonance) and 350 Hz, generating $F^+ = 4.2$ and $F^+ = 2.1$, respectively, and $\langle c_\mu \rangle$ was gradually increased. The jet deflection angles presented in Fig. 6 indicate a very low sensitivity to the forcing frequency in the range of frequencies tested. In the $\langle c_\mu \rangle$ range where the two F^+ overlap, the difference in the deflection angles is very small. Figure 6 also includes results obtained using the five-hole probe. These measurements agree very well with the shape of the hot-wire U velocity profiles (not shown) and provide deflection angles that are smaller by 0.5 to 1.25 deg [using Eq. (1b) rather than Eq. (3)]. This agreement is reasonable because Eq. (3) assumes that the jet started deflecting at $x = 0$ while Eq. (1b) does not require any assumption. The shape of the baseline and controlled velocity profiles are also insensitive to F^+. Examination of the velocity spectra where $U/U_e = 0.5$ (not shown) does not reveal any distinct frequencies with or without control. The power levels are almost identical below the excitation F^+, and the levels increase slightly above the excitation F^+. The lack of distinct peaks, even at the forcing frequencies, indicates that the excitation momentum was transferred to the mean flow and to smaller scales upstream of $x/D = 2.5$. The overall behavior of the jet response at different Re_D and excitation frequencies indicates low sensitivity to both Re_D and F^+ for this range of parameters.

3. *Effect of the Diffuser Length*

There is no consensus among researchers, regarding the relevant length scale that determines the effective forcing frequency, along with the velocity scale that is easily selected. One possibility is a local parameter based on the thickness of the shear layer, perhaps θ, its momentum thickness. Another option is the jet diameter. These two parameters dominate the near and far-field evolution of a transitional free jet, as identified by Drubka et al.[20] Presently, we introduce an additional length scale, the length of the diffuser. As demonstrated in Fig. 5 and will be further shown later, the presence of the diffuser significantly enhances the effectiveness of the streamwise excitation. The effect of the diffuser length was investigated using streamwise excitation and diffusers with $L/D = 0.58$, 1.0, and 1.85 corresponding to $F^+ = 1.3$, 2.3, and 4.2, respectively. F^+ was shown in the preceding section to have little effect on jet deflection angles over this range. Figure 8 shows the deflection angles vs $\langle c_\mu \rangle$ for the three diffuser lengths tested. The deflections measured using the $L = 0.58D$ diffuser were slightly lower than the deflections measured using the $L = 1.0D$ diffuser. The $L = 1.85D$, diffuser produced smaller deflections than the shorter diffusers at low $\langle c_\mu \rangle$. However, for $\langle c_\mu \rangle$ above 2% the longer diffuser ($L = 1.85D$) generated higher deflection angles. It is assumed that the diffuser length plays an important role in the nonlinear process leading to jet deflection through a feedback loop between the structures interacting with the diffuser exit and the excitation at the slot.

The mean velocity profiles for the three diffuser lengths (not shown, Ref. 19) indicate that the jet with the $L = 1.85D$ diffuser is more deflected on the side opposite the excitation slot and that

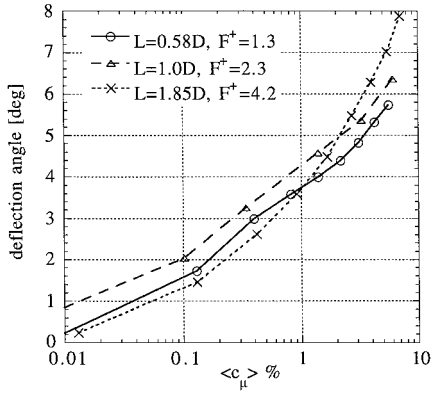

Fig. 8 Effect of varying the diffuser length L on jet deflection angles. $\phi = 30$ deg diffuser. $Re_D = 3.1 \times 10^4$, $x/D = 2.5$, and $z/D = 0.0$.

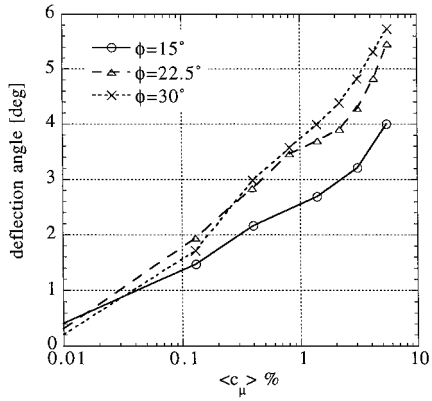

Fig. 9 Effect of varying the diffuser half-angle ϕ on jet deflection angles. $L = 0.58D$ diffuser. $Re_D = 3.1 \times 10^4$, $x/D = 2.5$, and $z/D = 0.0$.

less mixing takes place in the excited shear layer. This could be attributed to larger pressure forces and lower entrainment with the longer diffuser. The turbulence profiles (not shown) indicate that the jet velocity fluctuation level for the $L = 1.85D$ diffuser are higher in both shear layers and lower in the core of the jet.

4. Effect of the Diffuser Half-Angle

The effect of the diffuser half-angle ϕ was studied using streamwise excitation and diffusers with half-angles, $\phi = 15$, 22.5, and 30 deg, while fixing L at $0.58D$. Figure 9 shows jet deflection angles vs $\langle c_\mu \rangle$ for the three diffusers. Clearly, the $\phi = 15$ deg diffuser is the least effective of the three. The differences between the $\phi = 22.5$ deg diffuser and the $\phi = 30$ deg diffuser are small. The velocity profiles (not shown, Ref. 19) for $\langle c_\mu \rangle \cong 3\%$ indicate that the $\phi = 15$ deg diffuser is less effective at entraining flow on its excited side. The turbulence levels of the $\phi = 15$ deg diffuser are higher than the other two diffusers (not shown) on both shear layers. The differences between the U and u' profiles for the $\phi = 22.5$ deg and 30 deg diffusers are small, but still higher deflection angles as well as larger turbulence levels at the jet core were obtained using the diffuser with $\phi = 30$ deg.

5. Effect of the Excitation Direction

It is well known that where linear stability is valid and low-amplitude excitation is used the method of excitation is not important. At a certain distance from the source, typically a few wavelengths downstream, the excitation will be independent of the source details. On the other hand, when high-amplitude excitation is considered and nonlinearity plays an essential role, the source characteristics could dominate. This is especially important where the interaction between the controlled jet and the diffuser is a few wavelengths long. Two extreme options for the relative direction between the excitation and the jet flow were considered, the streamwise and

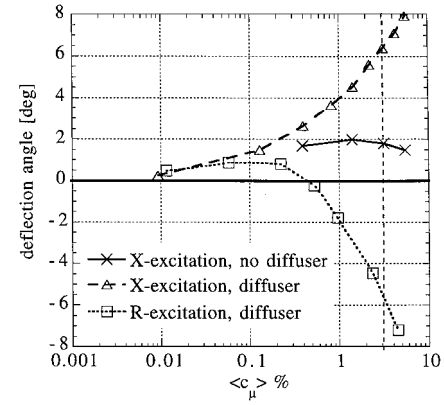

Fig. 10 Effect of excitation direction and presence of a diffuser on jet deflection angles. $L = 1.85D$ and $\phi = 30$ deg (when diffuser present). $Re_D = 3.1 \times 10^4$, $x/D = 2.5$, and $z/D = 0.0$. Vertical dashed line indicates profiles in Fig. 11.

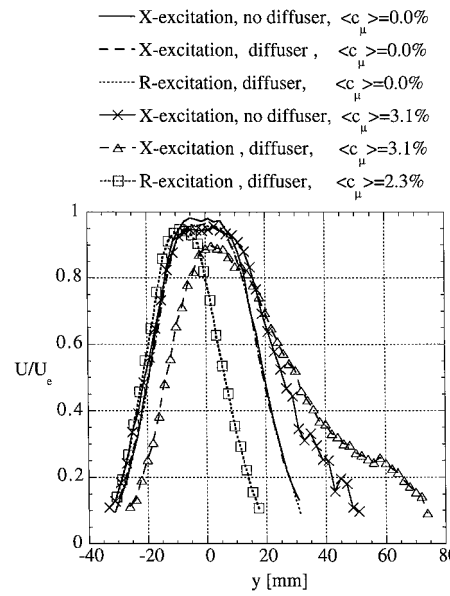

Fig. 11 U profiles showing effect of excitation direction and presence of diffuser on jet. $L = 1.85D$ and $\phi = 30$ deg (where diffuser present). $Re_D = 3.1 \times 10^4$, $x/D = 2.5$, and $z/D = 0.0$.

the cross-stream direction. As already shown, high-amplitude excitation deflects the jet toward (X-excitation, Fig. 5b) or away (R-excitation, Fig. 5c) from the excitation slot.

Jet deflection angles vs $\langle c_\mu \rangle$ for streamwise (X-excitation diffuser and no diffuser) and cross-stream (R-excitation) excitations are shown in Fig. 10. For small $\langle c_\mu \rangle$ the jet is deflected in the same direction (upward) for both types of excitation with a diffuser attached. The introduction of low $\langle c_\mu \rangle$ excitation into the upper shear layer causes enhanced spreading and interaction of that shear layer with the diffuser wall. As the level of $\langle c_\mu \rangle$ increases, the streamwise excitation continues to gradually deflect the jet upward toward the excited shear layer, while the jet is deflected away from the excitation slot when using cross-stream excitation with $\langle c_\mu \rangle$ greater than 0.5%. Note that both the X-excitation and the R-excitation are introduced through the slot surrounding the upper quarter of the jet circumference. Figure 11 shows a comparison of the mean velocity profiles for the baseline and controlled jet. The effect of introducing the excitation in the streamwise direction without a diffuser is only to increase the spreading rate of the excited shear layer. This was accompanied by significantly smaller jet deflection angles, compared to the deflection angles found for the X-excitation (Fig. 10). The streamwise excitation also causes enhanced spreading of the excited shear layer that interacts with the diffuser wall to deflect

the entire jet to that side (Fig. 11). High-level $\langle c_\mu \rangle$, introduced in the cross-stream direction, deflects the jet effectively away from the excitation slot, without enhancing its spreading rate in a comparable manner (see also Fig. 5c).

D. Response of the Jet to Pulsed Excitation

1. General

A wave packet is generated when a strong and concentrated disturbance, in both space and time, is introduced into an unstable shear layer. The concentrated excitation produces a complete spectrum of disturbance modes. The unstable shear layer will selectively amplify the most unstable modes and dampen the rest. This approach was first introduced by Gaster[21] to study linear instability of the Blasius boundary layer. Very good agreement between linear stability theory and experiments was found in the initial stages of transition. Gaster et al.[22] demonstrated that linear stability theory could also be applied to predict the evolution of two-dimensional harmonic wave trains introduced into a turbulent shear layer. Localized high-amplitude pulsed excitation generates turbulent spots in transitional boundary layers. Zilberman et al.[23] used an electric spark excitation to generate a turbulent spot and study its evolution in a fully turbulent boundary layer. A similar approach is presently used to study the frequency content, the effect of the excitation direction, the disturbance convection speed, and the relationship between the excitation and the nonlinear instability mechanism of the jet.

2. Experimental Details

A wave packet was generated by introducing a single cycle of the 700-Hz excitation through the slot surrounding the upper 90 deg of the jet circumference. The actuator and the data-acquisition sequence were triggered simultaneously. The data were sampled at 6 kHz, and 2500 records containing 512 points were acquired at each measurement station. The large number of data records was needed because of the low ratio between the wave-packet signal and the background turbulence. Data were acquired for two different excitation input levels that differed by about a factor of two in the amplitude of the pressure fluctuations, as measured in the actuator cavity. Data were acquired in the jet upper shear layer, where $U/U_e = 0.75$ at six axial locations $x/D = 0.1$, 0.2, 0.4, 0.8, 1.2, 1.6, inside the diffuser (when present). This was repeated three times: twice using a diffuser and excitation in the streamwise and cross-stream directions, and once more using streamwise excitation without a diffuser. Even though 2500 realizations were ensemble averaged, the low-amplitude wave-packet signal is hardly detectable (not shown). However, with the higher-amplitude excitation the wave packet is amplified and detectable.

3. Wave-Packet Results

The jet response to the high-amplitude pulsed excitation are shown in Figs. 12a–12c. Note that the perturbation signals are separated by $u'/U_e = 0.05$ for clarity. The resulting wave packets are clearly seen for all three jet exit configurations. For $x/D = 0.1$ and 0.2 and $t < 6$ msc, the signals are identical, showing the response to the one-cycle 700-Hz pulse. Further downstream, the excitation pulse decays and a low-frequency, high-amplitude disturbance develops. The amplitude of the wave packet generated by streamwise excitation (X-excitation, Fig. 12b) is the highest. The wave packet, generated in the absence of a diffuser (Fig. 12a), appears sooner at the measuring station and has only weak negative velocity perturbations in front of it. The cross-stream excited wave packet (Fig. 12c) is the least amplified of the three cases. The amplitude of the wave packet as a function of x was computed by integrating the time histories shown in Fig. 12. This amplitude Amp is expressed in terms of total fluctuating momentum in the form

$$\mathrm{AMP} = \int_{t=0}^{t=50\ \mathrm{ms}} \frac{u'^2}{U_e^2}\,\mathrm{d}t \tag{6a}$$

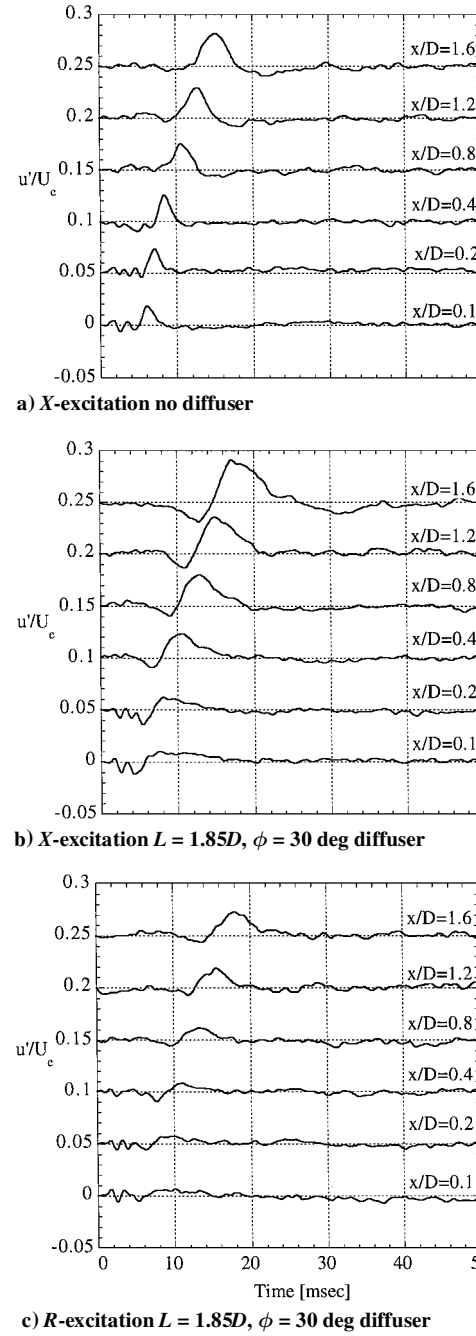

a) X-excitation no diffuser

b) X-excitation $L = 1.85D$, $\phi = 30$ deg diffuser

c) R-excitation $L = 1.85D$, $\phi = 30$ deg diffuser

Fig. 12 High-amplitude wave packets measured at various x/D, U/U_e = 0.75, and $Re_D = 3.1 \times 10^4$.

where the velocity perturbation $u'(t)$ is given by

$$u'(t) = U(t) - \frac{1}{T}\int_{t=50\ \mathrm{ms}}^{80\ \mathrm{ms}} U(t)\,\mathrm{d}t \tag{6b}$$

and the integration period T is 30 ms, after the response to the wave packet has passed. Integrating the perturbation momentum for $t > 50$ ms would only add noise. The peak amplitude of the wave packet can also be viewed as an indication of the mean flow distortion. Figure 13 shows how the total fluctuating momentum of the wave packet varies with x for the three jet-exit configurations examined. The initial fluctuating momentum is identical for the three configurations, indicating that the input is not sensitive to the presence of the diffuser or to the excitation direction. Figure 13 clearly shows that the disturbance resulting from the pulsed excitation in the streamwise direction (X-excitation) is the most amplified. The integrated fluctuating momentum for X-excited jet without a diffuser is less than a half its value with the diffuser present. This ratio

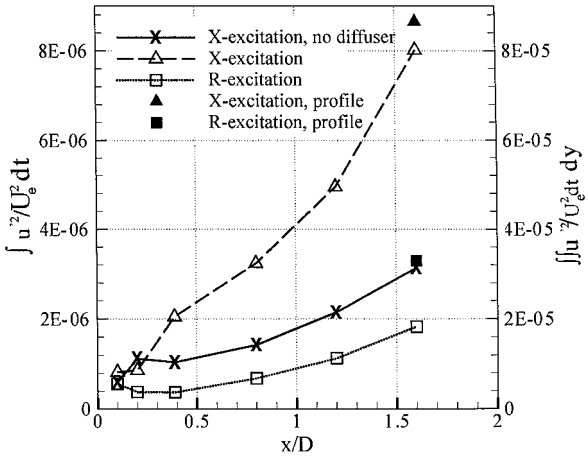

Fig. 13 Wave-packet amplitudes according to Eqs. (6). Conditions specified in Fig. 12.

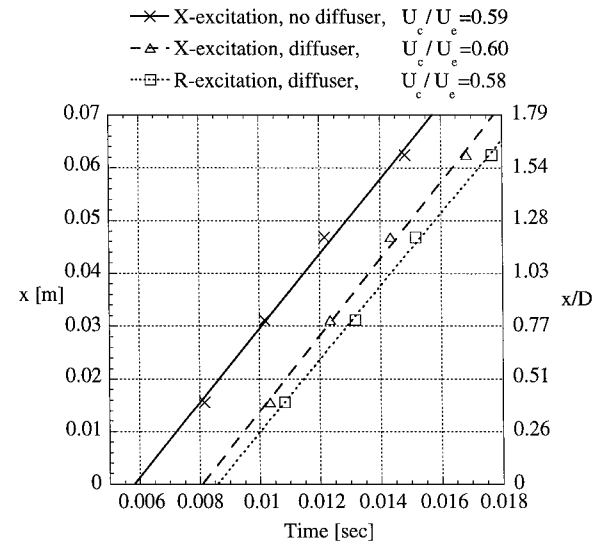

Fig. 14 Detection times of high-amplitude wave packet. Conditions specified in caption of Fig. 12.

decreases to almost a third at $x/D = 1.6$. The disturbance resulting from the cross-stream excitation is the least amplified. Further analysis, experimentation, and theoretical considerations are needed to clarify the physical mechanism leading to these differences. Wave-packet measurements were also made at $x/D = 1.6$, the diffuser exit, using streamwise and cross-stream excitation, across the entire y range of the jet at its plane of symmetry $z/D = 0.0$ (not shown, Ref. 19). The wave packet Amp integrated across the entire y range at $x/D = 1.6$ (filled symbols) are also shown in Fig. 13. The ratio of about three between the R and X modes indicates that the results presented in Fig. 13 for $U/U_e = 0.75$ are of a global nature. Furthermore, the data indicate that the wave packet generated by streamwise excitation is of significantly higher amplitude in the excited shear layer than in the nonexcited layer (3 and 0.5% respectively), whereas cross-stream excitation affects the entire jet cross section, generating comparable amplitudes in both shear layers. The maximum amplitude of the X-excitation wave packet is much higher than the maximum amplitude of the R-excitation wave packet. This demonstrates how much more receptive the excited shear layer is to streamwise excitation. It also shows that the cross-stream excitation generates a more global response rather than the response generated by the streamwise excitation that mainly affects the excited shear layer. This pattern clarifies why the jet is effectively vectored toward the excited shear-layer side when using the X-excitation (Fig. 10). It also indicates that the excitation using the R-excitation is not related to an instability mechanism, when high amplitude is applied. The mechanism responsible for the jet deflection away from the excitation slot, using cross-stream excitation, is presumably similar to the mechanism responsible for the modification in the jet cross section measured by Davis[3] using two steady control jets.

The convection speeds of the wave packet (Fig. 14) were computed by determining the wave-packet appearance time at each x location for the three types of high-amplitude excitation. The wave packet was thought to be in the initial stages of development at $x/D = 0.1$ and 0.2; therefore, these two points were omitted from the convection speed computations. All convection speeds were calculated by applying a linear fit to the data shown in Fig. 14. The convection speeds are 0.59 ± 0.01 of the jet-exit velocity. This value corresponds favorably with convection speeds of coherent structure in turbulent shear-layers[23] and with linear stability theory predictions (Ref. 20 and references therein). The convection speed of the wave packet generated by streamwise excitation is slightly higher, even though the mean flow speed is lower when the jet is spread more toward the excitation slot. It indicates that streamwise excitation should result in a faster response to changes in the excitation $\langle c_\mu \rangle$. The reason for the earlier appearance of the wave packet when there is no diffuser at the jet exit is not clear. It might be connected to slight differences in the nature of the interaction between the excitation and the shear layer very close to the excitation slot in the absence of the diffuser (i.e., more efficient entrainment).

Analyzing the frequency content of the wave packet reveals that the most amplified frequency for the free jet (no diffuser attached) is around 100 Hz. This frequency corresponds favorably with both shear-layer modes[20] $S_{t\theta} = 0.02$ and with the column mode $S_{tD} \sim 0.2$–0.6. However, the limited frequency scans performed (Fig. 6) indicate that the 350-Hz excitation did not generate higher deflection angles than the 700-Hz excitation in the range of parameters studied. The most amplified frequency is reduced to 50–70 Hz when a diffuser is attached. These frequencies combined with a phase velocity of $0.6U_e$ (evaluated from the convection speed that was calculated in Sec. III D, 3) result in a disturbance wavelength of about 3 jet diameters. It seems that this wavelength is too long to interact with a diffuser that is about half this length. Limited data gathered with a longer, $\phi = 22.5$ deg diffuser with streamwise excitation did not generate greater deflection angles, and practical considerations show preference to shorter diffusers.

E. Jet Response to Step Changes in $\langle c_\mu \rangle$

The response of the jet to step changes in the magnitude of the excitation $\langle c_\mu \rangle$ was also investigated. Studying the response of a system is a fundamental step in identifying the dynamics of the control process. For this investigation data were acquired with the actuator toggled between off, on, and off again. Detailed results are presented in Ref. 19. All measurements were made at an axial location corresponding to the diffuser exit $x/D = 1.6$ and the plane of symmetry of the excitation $z/D = 0.0$. In the cases where a diffuser was attached to the jet exit, the length of the diffuser L was $1.85D$, and the half-angle ϕ was 30 deg.

The Reynolds-number dependence of the response was studied by altering the jet-exit velocity and using streamwise excitation. The results for Reynolds numbers corresponding to $U_e = 8$, 12, and 18 m/s are presented in Figs. 15a and 15b for actuator on and off responses, respectively. The same $\langle c_\mu \rangle$ was maintained at all Re_D. Time is multiplied by U_e to provide a common convection length for the response. This normalization collapses the data very well, indicating Re_D insensitivity and a typical response time of $0.4/U_e$ seconds for the present geometry (U_e is given in m/s). Assuming that the convection speed is independent of Re_D, it is highly feasible that the jet will respond within a convection distance of about 3–4 diameters regardless of Re_D, jet diameter, and jet-exit velocity.

The fast response and its independence of Re_D are very encouraging for control purposes. However, the strong transients identified in the jet response, mainly of the streamwise excitation, are a concern from an application point of view and could be addressed by closed-loop control. This is especially important because the streamwise excitation is the most effective, as it requires the minimum $\langle c_\mu \rangle$ to generate effective spreading and vectoring at $\langle c_\mu \rangle$ levels of about

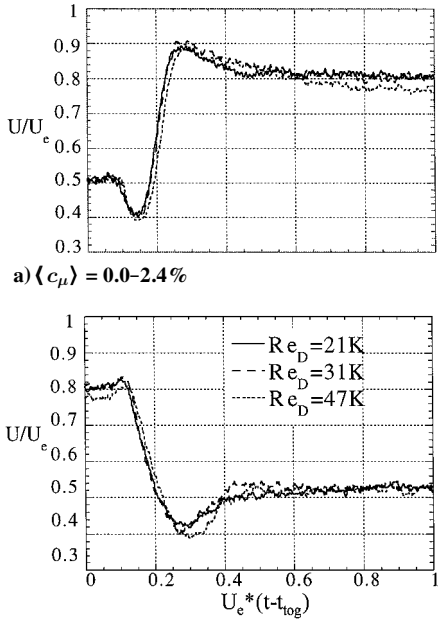

a) $\langle c_\mu \rangle$ = 0.0–2.4%

b) $\langle c_\mu \rangle$ = 2.4–0.0%

Fig. 15 Lack of Re_D effect on jet response to a step change in $\langle c_\mu \rangle$. x/D = 1.6, z/D = 0.0, U/U_e = 0.5, ϕ = 30 deg, L = 1.85D diffuser, X-excitation.

1%. This is probably the upper limit of what can be achieved in high subsonic speed applications.

IV. Summary and Conclusions

Periodic excitation was introduced through a slot surrounding the upper quarter of the circumference of a turbulent circular jet to vector it and enhance its spreading rate. A diffuser, attached to the jet exit, promoted attachment of the jet shear layer to the diffuser wall in a similar manner to that found in airfoil experiments using periodic excitation.

The boundary layer upstream of the jet exit was tripped to achieve turbulent flow at the jet exit. Data were acquired for Re_D between 1.6×10^4 and 4.7×10^4. The tripped boundary layers of the jet generated a Reynolds-number independent flow, the desired effect. The turbulence level in the jet core was 3% whereas in the shear layers it reached a maximum of 13%.

The use of periodic excitation and a diffuser at the jet exit in a flow control experiment introduced additional parameters such as frequency, excitation momentum and its direction, diffuser length, and diffuser half-angle. The jet deflection angles were insensitive to the excitation frequency, in the range of parameters studied. The jet deflection angles were independent of the Reynolds number, although some differences were noticed in the jet behavior at $Re_D = 2.1 \times 10^4$, close to the transition Re_D. Diffusers of length-to-diameter ratio between 0.58 and 1.85 were tested. The longest diffuser $L/D = 1.85$ generated somewhat higher deflection angles for $\langle c_\mu \rangle$ above 2%. Jet deflection angles were lower for a diffuser half-angle of 15 deg than for diffuser half-angles of 22.5 and 30 deg. Jet deflection was highly sensitive to the direction in which the excitation was introduced. Periodic excitation, introduced in the streamwise direction, vectored the jet toward the diffuser wall where the excitation was introduced. Low-amplitude excitation introduced in the cross-stream direction vectored the jet in the same direction, but high-amplitude excitation introduced in the cross-stream direction vectored the jet away from the wall where the excitation was introduced.

Pulsed excitation was used to generate wave packets in the jet shear layer in order to study the frequency content, the effect of the excitation direction, the disturbance convection speed, and the relationship between the excitation and an instability mechanism. These studies revealed that the presence of a diffuser at the jet exit significantly amplified the pulsed excitation introduced in the streamwise direction. The favorable interaction between the excitation, the jet flow, and the diffuser wall explains the higher jet deflection angles obtained with the diffuser when exciting the shear layer in the streamwise direction. The wave packet excited by introducing a pulsed excitation in the cross-stream direction evolved differently even though a diffuser was present. This wave packet is the least amplified among the cases studied. It is also of similar amplitude in both the excited and opposite shear layers, indicating a more global effect of the excitation when introduced in the cross-stream direction.

The jet responded quickly, on the order of 10–20 ms, to step changes in the level of the excitation. The response was independent of the Reynolds number when the jet-exit velocity was increased. The practical implication of this finding is that a proportional increase in dimensions and speed will maintain a similar response time.

From this jet control study a number of areas for future research were identified. One area is the use of simultaneous streamwise and cross-stream excitation on opposite sides of the jet. It is assumed that significantly higher jet deflection angles could be obtained this way. The effect of the diffuser on the cross-stream excitation has not been studied yet. More wave-packet studies, where diffusers of different lengths would be used, are required to better understand how the amplification and convection speed of the wave packet (and the associated mean flow distortion) are effected by the diffuser length. Finally, it is planned to use periodic excitation for the control of a rectangular jet with an exit diffuser. A rectangular jet is of interest because of the longer shear layers per unit area and the additional possible modes. One such mode is jet rotation.

A fast responding method of altering the direction of the flow emanating from a low-speed, turbulent circular jet was demonstrated. Moderate $\langle c_\mu \rangle$ were required to produce this effect. The technique could be applied to a number of applications including jet-engine exhaust, gust alleviation, and control surface augmentation or replacement without moving parts.

Acknowledgment

This work was performed while the second author held a National Research Council/NASA LaRC research associateship. The authors would like to thank W. L. Sellers III, M. J. Walsh, R. D. Joslin, G. B. Beeler, and C. B. McGinley for their support.

References

[1] Crow, S. C., and Champagne, F. H., "Orderly Structure in Jet Turbulence," *Journal of Fluid Mechanics*, Vol. 48, Pt. 3, 1971, pp. 547–591.

[2] Zaman, K. B. M. Q., and Hussain, A. K. M. F., "Turbulence Suppression in Free Shear Flows by Controlled Excitation," *Journal of Fluid Mechanics*, Vol. 103, 1981, pp. 133–159.

[3] Davis, M. R., "Variable Control of Jet Decay," *AIAA Journal*, Vol. 20, No. 5, 1982, pp. 606–609.

[4] Strykowski, P. J., and Wilcoxin, P. J., "Mixing Enhancement Due to Global Oscillations in Jets with Annular Counterflow," *AIAA Journal*, Vol. 31, No. 3, 1993, pp. 564–570.

[5] Strykowski, P. J., and Krothapalli, A., "The Countercurrent Mixing Layer: Strategies for Shear-Layer Control," AIAA Paper 93-3260, July 1993; also Krothapalli, A., Strykowski, P. J., and King, C. J., "Origin of Streamwise Vortices in Supersonic Jets," *AIAA Journal*, Vol. 36, No. 5, 1998, pp. 869–872.

[6] Strykowski, P. J., Krothapalli, A., and Forliti, D. J., "Counterflow Thrust Vectoring of Supersonic Jets," AIAA Paper 96-0115, Jan. 1996; also *AIAA Journal*, Vol. 34, No. 11, 1996, pp. 2306–2314.

[7] Raman, G., "Using Controlled Unsteady Fluid Mass Addition to Enhance Mixing," *AIAA Journal*, Vol. 35, No. 4, 1997, pp. 647–656.

[8] Smith, B. L., and Glezer, A., "Vectoring and Small-Scale Motions Effected in Free Shear Flows Using Synthetic Jet Actuators," AIAA Paper 97-0213, Jan. 1997.

[9] Huerre, P., and Monkewitz, P. A., "Absolute and Convective Instabilities in Free Shear Layers," *Journal of Fluid Mechanics*, Vol. 159, 1985, pp. 151–168.

[10] Viets, H., "Flip-Flop Jet Nozzle," *AIAA Journal*, Vol. 13, No. 10, 1975, pp. 1375–1379.

[11] Davis, S. A., and Glezer, A., "Mixing Control of Fuel Jets Using Synthetic Jet Technology: Velocity Field Measurements," AIAA Paper 99-0447, Jan. 1999.

[12]Smith, B. L., and Glezer, A., "The Formation and Evolution of Synthetic Jets," *Physics of Fluids*, Vol. 10, No. 9, 1998, pp. 2281–2297.

[13]Grinstein, F. F., and DeVore, C. R., "Entrainment and Thrust Vector Control with Countercurrent Rectangular Jets," AIAA Paper 99-0165, Jan. 1999.

[14]Seifert, A., Bachar, T., Koss, D., Shepshelovich, M., and Wygnanski, I., "Oscillatory Blowing, a Tool to Delay Boundary Layer Separation," *AIAA Journal*, Vol. 31, No. 11, 1993, pp. 2052–2060.

[15]Seifert, A., Darabi, A., and Wygnanski, I., "On the Delay of Airfoil Stall by Periodic Excitation," *Journal of Aircraft*, Vol. 33, No. 4, 1996, pp. 691–699.

[16]Seifert, A., and Pack, L. G., "Oscillatory Control of Separation at High Reynolds Numbers," *AIAA Journal*, Vol. 37, No. 9, 1999, pp. 1063–1071.

[17]Kinser, E., and Rediniotis, O. K., "Development of a Nearly-Omni-Directional, Three-Component Velocity Measurement Pressure Probe," AIAA Paper 96-0037, Jan. 1996.

[18]Hussain, A. K. M. F., and Zedan, M. F.,"Effects of the Initial Condition on the Axisymmetric Free Shear Layer: Effects of the Initial Momentum Thickness," *Physics of Fluids*, Vol. 21, No. 7, 1978, pp. 1100–1112.

[19]Pack, L. G., and Seifert, A., "Periodic Excitation for Jet Vectoring and Enhanced Spreading," AIAA Paper 99-0672, Jan. 1999.

[20]Drubka, R. E., Reisenthel, P., and Nagib, H. M., "The Dynamics of Low Initial Disturbance Turbulent Jet," *Physics of Fluids, A*, Vol. 1, No. 1, 1989, pp. 1723–1735.

[21]Gaster, M., "The Development of Three-Dimensional Wave Packets in a Boundary Layer," *Journal of Fluid Mechanics*, Vol. 32, 1968, pp. 173–184.

[22]Gaster, M., Kit, E., and Wygnanski, I., "Large-Scale Structures in a Forced Turbulent Mixing Layer," *Journal of Fluid Mechanics*, Vol. 150, 1985, pp. 23–39.

[23]Zilberman, M., Wygnanski, I., and Kaplan, R. E., "Transitional Boundary Layer Spot in a Fully Turbulent Environment," *Physics of Fluids*, Supplement 20, 1977, pp. S258–271.